2021 18th Annual IEEE International Conference on Sensing, Communication, and Networking (SECON) | 978-1-6654-4108-7/21/$31.00 ©2021 IEEE | DOI: 10.1109/SECON52354.2021.9491602

SwarmShare: Mobility-Resilient Spectrum Sharing for Swarm UAV Networking in the 6 GHz Band

Jiangqi Hu[1], Sabarish Krishna Moorthy[1], Ankush Harindranath[1], Zhangyu Guan[1],
Nicholas Mastronarde[1], Elizabeth Serena Bentley[2], and Scott Pudlewski[3]
[1]Department of Electrical Engineering, University at Buffalo, Buffalo, NY 14260, USA
[2]Air Force Research Laboratory (AFRL), Rome, NY 13440, USA
[3]Georgia Tech Research Institute (GTRI), Atlanta, GA 30332, USA
Email: {jiangqih, sk382, ankushha, guan, nmastron}@buffalo.edu,
elizabeth.bentley.3@us.af.mil, scott.pudlewski@gtri.gatech.edu

***Abstract*—To mitigate the long-term spectrum crunch problem, the FCC recently opened up the 6 GHz frequency band for unlicensed use. However, the existing spectrum sharing strategies cannot support the operation of access points in moving vehicles such as cars and UAVs. This is primarily because of the directionality-based spectrum sharing among the incumbent systems in this band and the high mobility of the moving vehicles, which together make it challenging to control the cross-system interference. In this paper we propose *SwarmShare*, a mobility-resilient spectrum sharing framework for swarm UAV networking in the 6 GHz band. We first present a mathematical formulation of the *SwarmShare* problem, where the objective is to maximize the spectral efficiency of the UAV network by jointly controlling the flight and transmission power of the UAVs and their association with the ground users, under the interference constraints of the incumbent system. We find that there are no closed-form mathematical models that can be used characterize the statistical behaviors of the aggregate interference from the UAVs to the incumbent system. Then we propose a data-driven three-phase spectrum sharing approach, including *Initial Power Enforcement*, *Offline-dataset Guided Online Power Adaptation*, and *Reinforcement Learning-based UAV Optimization*. We validate the effectiveness of *SwarmShare* through an extensive simulation campaign. Results indicate that, based on *SwarmShare*, the aggregate interference from the UAVs to the incumbent system can be effectively controlled below the target level *without* requiring the real-time cross-system channel state information. The mobility resilience of *SwarmShare* is also validated in coexisting networks with *no* precise UAV location information.**

I. Introduction

Unmanned aerial vehicles (UAVs) have been envisioned as a key technology for next-generation (i.e., B5G or 6G) wireless networks [1], [2]. Because of their features of fast deployment, high mobility and small size, UAVs have a great potential to enable a wide set of new applications, including UAV-aided guidance, small cells with flying base stations, emergency wireless networking in the aftermath of disasters, among others. The foreseen wide adoption of UAV systems can pose a significant burden on the capacity of the underlying wireless networks. In this paper we aim to explore new approaches that can enable UAV operations in the 6 GHz band to harvest the addtitional 1.2 GHz spectrum bandwidth [3].

The primary challenge towards this goal is in the spectrum sharing approaches adopted by the incumbent systems in this frequency band. The 6 GHz band consists of four sub-bands, i.e., U-NII-5 (5.925-6.425 GHz), U-NII-6 (6.425-6.525 GHz), U-NII-7 (6.525-6.875 GHz), and U-NII-8 (6.875-7.125 GHz). These bands have been previously occupied by a set of non-government services, including fixed point-to-point services, fixed-satellite service (Earth-to-space), broadcast auxiliary service and cable television relay service [3]. These incumbent systems coexist with each other by sharing the spectrum on a directional basis, i.e., they use highly directional antennas to concentrate the signal energy in a particular direction such that mutual interference can be effectively mitigated as long as their antennas are not pointed toward each other. As a result, traditional carrier-sensing-based spectrum sharing as in Wi-Fi networks is non-applicable to extend those wireless systems with omnidirectional antennas to this frequency band, because of the low detectability of the incumbent systems. For this reason, two operation modes have been proposed by the FCC, i.e., standard-power and low-power modes. The former allows both indoor and outdoor operations on the U-NII-5 and U-NII-7 bands with maximum transmission power of 30 dBm. The latter focuses on indoor operations in the U-NII-6 and U-NII-8 bands with maximum transmission power of 24 dBm.

However, none of the above two modes support UAV operations in the 6 GHz bands [3], [4]. A major concern is with the high mobility of the UAV systems, which makes it difficult to model and control their aggregate interference to the incumbent systems. The situation gets even worse when considering the altitude-dependent interference range of UAVs and the higher probability of line-of-sight signal propagation at higher altitudes. Additionally, it is also challenging for the distributed UAVs to control their aggregate interference

ACKNOWLEDGMENT OF SUPPORT AND DISCLAIMER: (a) Contractor acknowledges Government's support in the publication of this paper. This material is based upon work funded in part by AFRL under AFRL Contract No. # FA8750-20-1-0501 and in part by the NSF under Grant SWIFT-2030157. (b) Any opinions, findings and conclusions or recommendations expressed in this material are those of the author(s) and do not necessarily reflect the views of AFRL.

Distribution A. Approved for public release: Distribution unlimited : AFRL-2021-1038 on March 30, 2021.

collaboratively by jointly considering their spectrum access strategies and association to the ground users.

To address these challenges, a key step is to understand the statistical behaviors and effects of the aggregate interference experienced by the incumbent systems, since no real-time cross-system channel state information (CSI) is available. To this end, in this paper we focus on a new spectrum sharing scenario in the 6 GHz band called *SwarmShare*, where a set of UAVs collaboratively provide data streaming services to ground users, by sharing the spectrum with the incumbent systems on the 6 GHz band under the cross-system interference constraints. Within this framework, we model and analyze the aggregate interference from the UAVs to the incumbent, and propose a mobility-resilient stochastic spectrum sharing approach. The main contributions of this work are as follows:

- We first present a mathematical formulation of the *SwarmShare* problem, where the objective is to maximize the spectral efficiency of the wireless UAV network by jointly controlling the UAVs' transmission power and flight trajectory as well as their association to the ground users, under the interference constraints of the incumbent system. It is shown that the resulting problem is a mixed integer nonlinear non-convex programming (MINLP) problem.
- We analyze the statistical behavior of the aggregate interference from the UAVs to the incumbent system, and find that no existing models can be used to characterize the statistical behavior of the interference. With this observation, we propose to solve the above MINLP spectrum sharing problem following a data-driven three-phase approach: *Initial Power Enforcement*, *Offline-dataset Guided Online Power Adaptation*, and *Reinforcement Learning-based UAV Optimization*.
- We validate the effectiveness of *SwarmShare* by conducting an extensive simulation campaign over UBSim, a newly developed Universal Broadband Simulator for integrated aerial-ground wireless networks. It is found that, with *SwarmShare*, effective spectrum sharing can be achieved *without* real-time cross-system channel state information, and, which is somewhat surprising, even with *no* precise location information of the UAVs.

The rest of the paper is organized as follows. In Section II, we discuss the related works. The system model and problem formulation is presented in Section III. In Section IV, we describe the spectrum sharing framework. Performance evaluation results are discussed in Section V and finally we draw the main conclusions in Section VI.

II. Related Work

UAV systems have attracted significant research attention in both academia and industry [1], [5]–[8]. For example, in [1] the authors optimize the achievable rate of UAV-aided cognitive IoT networks. Wang et al. propose in [5] a dynamic hyper-graph coloring approach for spectrum sharing in UAV-assisted networks. In [6], the authors optimize mobile terminals' throughput by jointly controlling UAV trajectory, bandwidth allocation and user partitioning between the UAV and ground base stations. In [7], UAV is used as relay to assist D2D communications. [8] studies machine learning based spectrum sharing for UAV-assisted emergency communications. Readers are referred to [9] and references therein for a survey of the main results in this area.

Spectrum sharing in cognitive radio networks has also been a hot research topic for a long time with a sizable and increasing body of literature. In [10], the authors aim to maintain network connectivity in cognitive radio networks by controlling the transmission power of sensors. In [11], the authors maximize the revenue of the newly joined systems in cognitive radio networks by controlling the channel access of new users. The authors of [12] propose a cognitive backscatter network to maximize the data rate of the newly joined networks.

Spectrum sharing between directional- and omnidirectional-antenna wireless systems has also been studied in existing literature. For example, [13] optimizes the performance of LTE-Unlicensed networks while guaranteeing the performance of the co-located radar system. The authors of [14] propose RadChat, a distributed networking protocol for mitigation of interference among frequency modulated continuous wave radars. A cooperative spectrum sharing model is proposed in [15] to mitigate the mutual interference among radar and communication system. Please refer to [16] and references therein for a good survey of the main results in this field.

Different from the above discussed works, none of which have considered the spectrum sharing between UAVs and the incumbent wireless systems in the 6 GHz band, in this paper we aim to *design a new, mobility-resilient spectrum sharing framework to enable wireless UAV networking in this band.*

III. System Model and Problem Formulation

We consider a wireless UAV network coexisting with an incumbent communication pair Tx and Rx by sharing the same portion of spectrum B in the 6 GHz band. The UAV network consists of a set $\mathcal{K}$ of UAVs collaborating with each other to serve a set $\mathcal{M}$ of ground users. The transmission time is divided into a set $\mathcal{T}$ of consecutive time slots. In each time slot $t \in \mathcal{T}$, denote the coordinate vector of UAV $k \in \mathcal{K}$ as $\mathbf{cod}_k^t = [x_k^t, y_k^t, z_k^t]^{\mathrm{T}}$, with T being the transpose operation and x_k^t, y_k^t and z_k^t representing the x-, y- and z-axis components, respectively. Similarly, denote respectively $\mathbf{cod}_{\mathrm{Tx}} = [x_{\mathrm{Tx}}, y_{\mathrm{Tx}}, z_{\mathrm{Tx}}]^{\mathrm{T}}$, $\mathbf{cod}_{\mathrm{Rx}} = [x_{\mathrm{Rx}}, y_{\mathrm{Rx}}, z_{\mathrm{Rx}}]^{\mathrm{T}}$ and $\mathbf{cod}_i = [x_i, y_i, z_i]^{\mathrm{T}}$ as the coordinate vectors of incumbent transmitter Tx, incumbent receiver Rx and ground node $i \in \mathcal{M} \cup \{\mathrm{Tx}, \mathrm{Rx}\}$. Denote $\mathcal{A} = \mathcal{K} \cup \mathcal{M} \cup \{\mathrm{Tx}, \mathrm{Rx}\}$ as the set of all the nodes in the heterogeneous network. The objective of the UAV network is to maximize its own spectral efficiency under the interference constraints of the incumbent system. Before presenting the formal formulation of the spectrum sharing problem, we first describe the considered channel, antenna and throughput models.

A. Channel Model

We consider both large-scale path-loss and small-scale fading. For path-loss, we consider line-of-sight (LoS) wireless channels between the incumbent transmitter Tx and its receiver Rx. This is feasible because the incumbent systems are usually carefully deployed such that their antennas are well-aligned without any obstructions in the link. However, we consider non-line-of-sight (NLoS) links between the incumbent nodes and the ground users of the coexisting networks. For UAV network, we consider as in [17] a probabilistic path-loss model for the links between UAVs and ground nodes. Then, the LoS and NLoS path-loss (in dB) between UAV $k \in \mathcal{K}$ and ground node $i \in \mathcal{M} \cup \{\mathrm{Tx}, \mathrm{Rx}\}$ can be given as, in time slot $t \in \mathcal{T}$,

$$H_{ki}^{\mathrm{LoS},t} = 20\log\left(\frac{4\pi d_{ki}^t f}{c}\right) + \eta^{\mathrm{LoS}}, \tag{1}$$

$$H_{ki}^{\mathrm{NLoS},t} = 20\log\left(\frac{4\pi d_{ki}^t f}{c}\right) + \eta^{\mathrm{NLoS}}, \tag{2}$$

where the first item on the righ-hand side of (1) and (2) represents the free space path-loss with $d_{ki}^t = ||\mathbf{cod}_k^t - \mathbf{cod}_i||_2$ being the distance between UAV k and receiver i in time slot t, f is the carrier frequency of UAV k, c is the speed of light, and η^{LoS} and η^{NLoS} are the additional attenuation factors due to LoS and NLoS transmissions, respectively. Let $\Pr(H_{ki}^{\mathrm{LoS},t})$ represent the probability of LoS transmissions in time slot t, then $\Pr(H_{ki}^{\mathrm{LoS},t})$ can be expressed as [18],

$$\Pr(H_{ki}^{\mathrm{LoS},t}) = (1 + X\exp\left(-Y[\phi_{ki} - X]\right))^{-1}, \tag{3}$$

where X and Y are given environment-dependent constants and $\phi_{ki} = \sin^{-1}(z_k^t/d_{ki}^t)$. Accordingly, the probability of NLoS transmissions between UAV $k \in \mathcal{K}$ and receiver $i \in \mathcal{M} \cup \{\mathrm{Tx}, \mathrm{Rx}\}$ can be given as $\Pr(H_{ki}^{\mathrm{NLoS},t}) = 1 - \Pr(H_{ki}^{\mathrm{LoS},t})$.

Finally, for small-scale fading we consider Rician fading for LoS transmissions and Rayleigh fading for NLoS. Denote K_{ij} as the Rician factor for the wireless channel between nodes $i, j \in \mathcal{A}$, then K_{ij} can be given as $K_{ij} = 13 - 0.03d_{ij}$ for LoS transmissions and 0 for NLoS, where d_{ij} is the distance between the two nodes. Denote the resulting small-scale fading coefficient as $h_{ij}^t \triangleq h_{ij}^t(K_{ij})$ for nodes $i, j \in \mathcal{A}$.

B. Antenna Model

As described in section I, in this work we consider directional transmissions for the incumbent wireless systems and omnidirectional transmissions for the coexisting UAV network. Specifically, we consider as in [19] bi-sectorized antenna model to characterize the interference between directional and omnidirectional antennas. Denote θ_{Tx} and θ_{Rx} as the signal beamwidth of the incumbent transmitter and receiver's antennas, respectively. Let $\theta_m \in [-\pi, \pi]$ denote the offset angle of the boresight direction of the Tx's antenna with respect to the reference direction for ground user $m \in \mathcal{M}$. Here, the reference direction refers to the direction along which the Tx's antenna would be exactly pointed to user m. Then the antenna gain of incumbent transmitter Tx with respect to ground user $m \in \mathcal{M}$ in time slot t, denoted as $w_{m\mathrm{Tx}}^t$, can be written as

$$w_{m\mathrm{Tx}}^t = \begin{cases} w_{\mathrm{Tx}}^{\max}, & \text{if } \theta_m \le \theta_{\mathrm{Tx}} \\ w_{\mathrm{Tx}}^{\min}, & \text{otherwise} \end{cases}, \tag{4}$$

where $w_{\mathrm{Tx}}^{\max}$ and $w_{\mathrm{Tx}}^{\min}$ represent the maximum and minimum transmit gains of the incumbent transmitter, respectively. Similarly, the receive gain of the incumbent receiver Rx with respect to UAV $k \in \mathcal{K}$, denoted as $w_{k\mathrm{Rx}}^t$, can be given as

$$w_{k\mathrm{Rx}}^t = \begin{cases} w_{\mathrm{Rx}}^{\max}, & \text{if } \theta_k \le \theta_{\mathrm{Rx}} \\ w_{\mathrm{Rx}}^{\min}, & \text{otherwise} \end{cases}, \tag{5}$$

with $w_{\mathrm{Rx}}^{\max}$ and $w_{\mathrm{Rx}}^{\min}$ being the maximum and minimum receive gains of the incumbent receiver, respectively. The transmit and receive gains are set to the maximum values for incumbent transmissions, i.e., $w_{\mathrm{Tx}}^{\max}$ and $w_{\mathrm{Rx}}^{\max}$, respectively.

C. Throughput Model

Based on the above channel and antenna models, the signal-to-interference-plus-noise ratio (SINR) of the incumbent receiver Rx, denoted as γ_{RX}^t for time slot t, can be written as

$$\gamma_{\mathrm{RX}}^t = \frac{p_{\mathrm{Tx}} w_{\mathrm{Tx}}^{\max} w_{\mathrm{Rx}}^{\max} \cdot (h_{\mathrm{TxRx}}^t)^2 / H_{\mathrm{TxRx}}^{\mathrm{LoS}}}{\sum\limits_{k\in\mathcal{K}} p_k^t w_{k\mathrm{Rx}}^t w_k \cdot (h_{k\mathrm{Rx}}^t)^2 / H_{k\mathrm{Rx}}^t + (\sigma_{\mathrm{Rx}})^2} \tag{6}$$

where p_{Tx} and p_k^t represent the transmission power of the incumbent transmitter Tx and UAV $k \in \mathcal{K}$ in time slot $t \in \mathcal{T}$, respectively; w_k denotes the transmit gain of the UAV and is considered to be constant for omnidirectional antennas; and $(\sigma_{\mathrm{Rx}})^2$ is the power of Additive White Gaussian Noise (AWGN) at the incumbent receiver.

The objective of *SwarmShare* is to guarantee satisfactory SINR for the incumbent system (i.e., γ_{RX}^t above) by controlling the transmission power of the coexisting UAVs. To this end, we consider single-home association strategy for the ground users of the UAV network, that is in each time slot $t \in \mathcal{T}$ each ground user can be served by at most one UAV. Denote α_{km} as the association variable, with $\alpha_{km} = 1$ if ground user $m \in \mathcal{M}$ is associated with UAV $k \in \mathcal{K}$ and $\alpha_{km} = 0$ otherwise. Then we have

$$\sum_{k\in\mathcal{K}} \alpha_{km}^t \le 1, \forall k \in \mathcal{K}, m \in \mathcal{M}, t \in \mathcal{T} \tag{7}$$

$$\alpha_{km}^t \in \{0, 1\}, \forall k \in \mathcal{K}, m \in \mathcal{M}, t \in \mathcal{T} \tag{8}$$

Denote $\mathcal{M}_k^t \triangleq \{m | m \in \mathcal{M}, \alpha_{km}^t = 1\}$ as the set of ground users served by UAV k in time slot t.

We further consider FDMA-based spectrum access among the UAVs in $\mathcal{K}$ and TDMA for the ground users served by the same UAV. Then, the SINR of ground user $m \in \mathcal{M}$ in time slot t, denoted as $\gamma_m^t = \gamma_m^t(H_{m\mathrm{Tx}}^t)$ can be expressed as

$$\gamma_m^t = \frac{p_{k(m)}^t \cdot (h_{k(m)m}^t)^2 / H_{k(m)m}^t}{(p_{\mathrm{Tx}}/|\mathcal{K}|) \cdot w_{m\mathrm{Tx}}^t \hat{w}_m \cdot (h_{m\mathrm{Tx}}^t)^2 / (H_{m\mathrm{Tx}}^t) + \sigma_m^2}, \tag{9}$$

where $k(m)$ and $\hat{w}_m$ represent the serving UAV and receive gain of ground user m, respectively; $|\mathcal{K}|$ denotes the number of UAVs in $\mathcal{K}$; $H_{k(m)m}^t \in \{H_{k(m)m}^{\mathrm{NLoS},t}, H_{k(m)m}^{\mathrm{LoS},t}\}$ is the path-loss from UAV $k(m)$ to ground user m in time slot t with $H_{k(m)m}^{\mathrm{NLoS},t}$ and $H_{k(m)m}^{\mathrm{LoS},t}$ defined in Section III-A; and σ_m^2 is the power of the AWGN noise at ground user m. Notice in (9) that

only $\frac{1}{|\mathcal{K}|}$ of the incumbent transmitter's power (i.e., $p_{\mathrm{Tx}}/|K|$) is considered for each UAV and its associated ground users because of the UAVs' FDMA-based spectrum access. It is worth pointing out that we consider FDMA- and TDMA-based spectrum access for the UAV networks because we want to focus this work on the interference control between the UAV and the incumbent systems. The resulting cross-system spectrum sharing scheme can also be extended to other more advanced spectrum access schemes for UAVs [20], [21].

Finally, the capacity achievable by user m in time slot t, denoted as $C^t_{k(m)m}$, can be expressed as

$$C^t_{k(m)m} = \frac{B}{|\mathcal{K}||\mathcal{M}^t_k|}\big[\Pr\left(H^{\mathrm{NLoS},t}_{k(m)m}\right)\log_2\left(1+\gamma^t_m(H^{\mathrm{NLoS}}_{k(m)m})\right) + \Pr\left(H^{\mathrm{LoS},t}_{k(m)m}\right)\log_2\left(1+\gamma^t_m(H^{\mathrm{LoS}}_{k(m)m})\right)\big], \quad (10)$$

where $\Pr(\cdot)$ is the probability of LoS and NLoS transmissions defined in Section III-A and $\gamma^t_m(\cdot)$ is the SINR of ground user m defined in (9).

D. Problem Formulation

Define $\mathbf{P} = (p^t_k)^{t\in\mathcal{T}}_{k\in\mathcal{K}}$ as the transmission power vector of the UAVs, $\mathbf{A} = (\alpha^t_{km})^{t\in\mathcal{T}}_{k\in\mathcal{K},m\in\mathcal{M}}$ as the UAV-user association vector, and $\mathbf{Q} = (\mathbf{cod}^t_k)^{t\in\mathcal{T}}_{k\in\mathcal{K}}$ as the UAV location vector. Then the objective of the *SwarmShare* control problem is to maximize the aggregate capacity of the UAV network by jointly controlling the transmission power of the UAVs and their flight trajectory as well as association with the ground users, while meeting the cross-system interference constraints, as formulated as

$$\underset{\mathbf{P},\mathbf{A},\mathbf{Q}}{Maximize} \ \frac{1}{|\mathcal{T}|}\sum_{t\in\mathcal{T}}\sum_{m\in\mathcal{M}} C^t_{k(m)m} \quad (11)$$

$$\text{Subject to}: \ 0 \le p^t_k \le p_{\max}, \forall k\in\mathcal{K}, t\in\mathcal{T}, \quad (12)$$

$$Association\ Constraints\ (7),\ (8) \quad (13)$$

$$\underbrace{\frac{1}{|\mathcal{T}|}\sum_{t\in\mathcal{T}}\mathrm{I}(\gamma^t_{\mathrm{Rx}} \le \gamma^{\mathrm{th}}_{\mathrm{Rx}}) \le \mathrm{Pr}^{\max}_{\mathrm{Rx}}}_{Cross-system\ Interference\ Constraint} \quad (14)$$

where $C^t_{k(m)m}$ is defined in (10), $p_{\max}$ is the maximum transmission power of each UAV, $\mathrm{I}(\cdot)$ is the indication function taking value of 1 if the condition holds and 0 otherwise, and $\gamma^{\mathrm{th}}_{\mathrm{Rx}}$ and $\mathrm{Pr}^{\max}_{\mathrm{Rx}}$ denote threshold SINR and the maximum tolerable SINR outage probability of the incumbent system.

IV. Spectrum Coexistence Design

The *SwarmShare* problem formulated in (11)-(14) is a mixed integer nonlinear nonconvex programming (MINLP) problem, because of the binary UAV-user association variables α^t_{km} and the underlying complicated mathematical expressions in (11) and (14). Moreover, to solve the problem directly it requires to know the real-time channel state information (CSI) between the UAV network and the incumbent system, which is however unavailable, as discussed in Section I, because of the low-detectability of the directional incumbent signals.

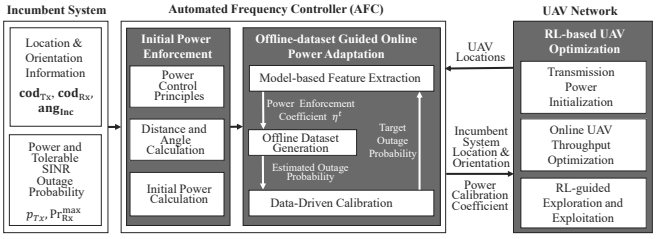

Fig. 1: *SwarmShare* Spectrum Sharing Framework.

To address the above challenges, in this work we consider an AFC (Automated Frequency Controller)-assisted spectrum sharing. AFC has been adopted for spectrum sharing in the TV whitespace band as well as the 6 GHz band by determining certain exclusion zones nearby the incumbent systems [3]. Our work differs from this with our objective to enable exclusion-zone-free hence more flexible spectrum sharing, and study the statistical behavior of the aggregate interference from the UAV networks to the incumbent system, while keeping the cross-system signaling at a minimum level. The diagram of the proposed spectrum coexistence framework is illustrated in Fig. 1, where there are three major components, i.e., *Initial Power Enforcement*, *Offline-dataset Guided Online Power Adaptation*, and *Reinforcement Learning-based UAV Optimization*.

A. Initial Power Enforcement

The objective of this phase is to determine, following a set of *Power Control Principles*, a rough transmission power for each of the UAVs. In this work, we consider three basic principles to accommodate the effects of the UAVs' flight altitude and their locations on the interference to the incumbent system, while more sophisticated principles can be incorporated in the future. These principles are i) UAVs that are closer to the incumbent receiver should transmit at lower power; (ii) with the same distance to the incumbent receiver, UAVs flying higher should transmit at lower power; and (iii) with the same distance and altitude, UAVs with smaller angles relative to the boresight axis of the incumbent receivers' directional antenna should transmit at lower power. Particularly, the rationale of the second principle is that, with the hybrid LoS/NLoS channel model described in Section III-A, it is more likely for a UAV to establish LoS links to the incumbent receiver when flying higher and hence cause more interference. Similarly, for the third principle, based on the directional antenna model described in Section III-B, a UAV will cause higher interference when more aligned with the incumbent receiver's antenna.

In *SwarmShare*, an initial power enforcement coefficient, denoted as $\mathrm{Enf}(\mathbf{cod}^t_k, \mathbf{cod}_{\mathrm{Rx}}, \mathbf{ang}_{\mathrm{Inc}})$, will be calculated for each UAV $k\in\mathcal{K}$ in time slot $t\in\mathcal{T}$ based on the above three principles. This is accomplished using three Sigmoid-family functions $Sig_1(\cdot)$, $Sig_2(\cdot)$ and $Sig_3(\cdot)$, as follows:

$$\mathrm{Enf}(\mathbf{cod}^t_k, \mathbf{cod}_{\mathrm{Rx}}, \mathbf{ang}_{\mathrm{Rx}}) = \underbrace{Sig_1\left(\frac{l_{\mathrm{euc}}(\mathbf{cod}^t_k, \mathbf{cod}_{\mathrm{Rx}})}{l^{\mathrm{th}}_{\mathrm{euc}}}\right)}_{Principle\ 1} \cdot \underbrace{Sig_2\left(\frac{h(\mathbf{cod}^t_k)+h(\mathbf{cod}_{\mathrm{Rx}})}{l^{\mathrm{th}}_{\mathrm{hgh}}}\right)}_{Principle\ 2} \cdot \underbrace{Sig_3\left(l_{\mathrm{rad}}(\mathbf{cod}^t_k, \mathbf{cod}_{\mathrm{Rx}}, \mathbf{ang}_{\mathrm{Inc}})\right)}_{Principle\ 3}, \quad (15)$$

where $l_{\rm euc}(\cdot,\cdot)$ represents the Euclidean distance between UAV k and the incumbent receiver given their coordinates; $h(\cdot)$ represents their height, and $l_{\rm rad}(\cdot,\cdot,\cdot) \in [0,\pi]$ is the angle (in radians) of UAV k with respect to the boresight axis of the incumbent receiver antenna; finally, $l_{\rm euc}^{\rm th}$ and $l_{\rm hgh}^{th}$ in equation (15) are respectively threshold distance and height beyond which $Sig_1(\cdot)$ and $Sig_2(\cdot)$ become nearly constant. It is worth pointing out that, since a standard sigmoid function is a differentiable, monotonically increasing, real function taking values in $[0,1]$, we design $Sig_1(\cdot)$, $Sig_2(\cdot)$ and $Sig_3(\cdot)$ by scaling, shifting and reversing the standard sigmoid function to consider the effects of UAV location, flight altitude and relative angle to the incumbent receiver. For example, $Sig_1(x) = \frac{1}{1+e^{-3(x/70-2)}}$ has been adopted for principle 1 in this work, while $Sig_2(\cdot)$ and $Sig_3(\cdot)$ can be defined similarly. With the obtained power enforcement coefficient $\mathrm{Enf}(\mathbf{cod}_k^t, \mathbf{cod}_{\rm Rx}, \mathbf{ang}_{\rm Inc})$, each UAV's power can be initialized as, in time slot $t \in \mathcal{T}$,

$$p_k^{\rm ini} = p^{\max}\mathrm{Enf}(\mathbf{cod}_k^t, \mathbf{cod}_{\rm Rx}, \mathbf{ang}_{\rm Inc}),\ \forall k \in \mathcal{K}, \tag{16}$$

where $p^{\max}$ is the maximum transmission power of each UAV.

B. Offline-dataset Guided Online Power Adaptation

Recall in Section III that our goal is to enable UAV operations in the 6 GHz band while meeting the cross-system interference constraint (14). In *SwarmShare*, this is accomplished by fine tuning the above obtained initial transmission powers for the UAVs following a three-step approach, as described as follows.

1) Model-based Feature Extraction: In this step, we first extract the network features that can be used later in *Data-Driven Calibration*, rather than using directly the raw network topology information such as UAV location vector $(\mathbf{cod}_k^t)_{k\in\mathcal{K}}^{t\in\mathcal{T}}$. This is important to mitigate the curse of dimensionality problem [22] especially with large number of UAVs. In *SwarmShare*, we select the power adaptation coefficient, denoted as η^t for time slot t, as the network feature. Then, given the above obtained initial transmission power $p_k^{\rm ini}$ for UAV $k \in \mathcal{K}$, a new transmission power p_k^t can be calculated as

$$p_k^t = p_k^{\rm ini}\eta^t \tag{17}$$

and interference constraint (14) can be rewritten as

$$\frac{1}{|\mathcal{T}|}\sum_{t\in\mathcal{T}} \mathrm{I}(\gamma_{\rm Rx}^t(\eta^t) \le \gamma_{\rm Rx}^{\rm th}) \le \mathrm{Pr}_{\rm Rx}^{\max}, \tag{18}$$

where $\gamma_{\rm Rx}^t(\eta^t)$ is the SINR of the incumbent receiver defined in (6) by substituting (17) into (6). Consider ergodic stochastic process for the aggregate interference and denote $\mathrm{Prob}\big(\gamma_{\rm Rx}^t(\eta^t) \le \gamma_{\rm Rx}^{\rm th}\big)$ as the SINR outage probability in time slot $t \in \mathcal{T}$, then the left-hand side of (18) can be equivalently represented as

$$\mathrm{Prob}\big(\gamma_{\rm Rx}^t(\eta^t) \le \gamma_{\rm Rx}^{\rm th}\big) \tag{19}$$

$$= \mathrm{Prob}\left(\frac{P_{\rm Rx}^{\rm sig}}{P_{\rm Rx}^{\rm itf}} \le \gamma_{\rm Rx}^{\rm th}\right) \tag{20}$$

$$= \int_0^{+\infty}\int_{\frac{P_{\rm Rx}^{\rm sig}}{\gamma_{\rm Rx}^{\rm th}}}^{+\infty} \underbrace{\mathrm{pdf}_{P_{\rm Rx}^{\rm sig}}(p^{\rm sig})}_{\substack{Noncentral\\ Chi-square\\ Distribution}} \cdot \underbrace{\mathrm{pdf}_{P_{\rm Rx}^{\rm itf}}(p^{\rm itf})}_{\substack{Gamma\\ Distribution}} \mathrm{d}p^{\rm itf}\mathrm{d}p^{\rm sig}, \tag{21}$$

where $P_{\rm Rx}^{\rm sig}$ and $P_{\rm Rx}^{\rm itf}$ are the numerator and denominator of (6), respectively; Rayleigh distribution has been considered for the small-scale fading and hence noncentral chi-square distribution [23] for the receive power of the incumbent signals; and finally as in [24], [25] Gamma distribution is considered for the aggregate interference power. The details of mathematical equations are omitted for the distributions due to space limitations. It is worth pointing out that, as shown later in Section V, the aggregate interference of UAVs does not follow any existing statistical distributions. In this work, we consider Gamma distribution in (21) because we want to obtain a rough estimation of the power adaptation coefficient η^t, which will be further calibrated based on offline dataset. Notice that given the maximum tolerable SINR outage probability $\mathrm{Pr}_{\rm Rx}^{\max}$ in (18), the maximum η^t can be determined efficiently by bisection search, since the left-hand side of (18), which is equivalent to (21), is a monotonically increasing function of the UAVs' transmission power hence η^t.

2) Offline-dataset Generation: Given the above obtained network feature η^t, and each UAV's transmission power p_k^t can be updated according to (17). Since the power adaptation may be inaccurate because of the inaccuracy of the Gamma distribution-based interference model in (21), we further calibrate the power control for UAVs with the assistance of offline measurements. Specifically, given the transmission power vector $(p_k^t)_{k\in\mathcal{K}}$, the corresponding SINR outage probability of the incumbent system can be obtained by offline simulations. By varying the number of UAVs, their locations as well as the maximum tolerable SINR outage probability in the simulations, we are able to obtain an SINR outage probability vector. Denote $\mathbf{Pr}_{\rm Rx}^{\max} = (\mathrm{Pr}_{\rm Rx}^{\max})$ as the vector of the maximum tolerable outage probability, and accordingly denote the simulated outage probability vector as $\overline{\mathbf{Pr}}_{\rm Rx}^{\max}(\boldsymbol{\eta}) = (\overline{\mathrm{Pr}}_{\rm Rx}^{\max}(\eta^t))$ with $\overline{\mathrm{Pr}}_{\rm Rx}^{\max}(\eta^t)$ being the SINR outage probability given network metric η^t and $\boldsymbol{\eta} = (\eta^t)$ the network feature vector.

3) Data-Driven Calibration: Finally, a mapping between $\mathbf{Pr}_{\rm Rx}^{\max}$ and $\overline{\mathbf{Pr}}_{\rm Rx}^{\max}(\boldsymbol{\eta})$ can be established through function approximation, e.g., based on linear regression [26], echo state learning [27] or deep neural networks [28]. In this work we find that it is enough to approximate the mapping based on linear regression. Denote the mapping as $\mathrm{Pr}_{\rm Rx}^{\max} = f(\overline{\mathrm{Pr}}_{\rm Rx}^{\max}(\eta^t))$. Then, given $\overline{\mathrm{Pr}}_{\rm Rx}^{\max}$, the value of $\mathrm{Pr}_{\rm Rx}^{\max}$ and the corresponding network feature η^t can be obtained at network run time and further used for UAV power control based on (17).

C. Reinforcement Learning-based UAV Optimization

As illustrated in Fig. 1, the above obtained η^t will be broadcast to the UAVs, which will then calculate their transmission power based on (17). Meanwhile, the UAVs will update their

flight and association strategies to serve their users with higher spectral efficiency. To this end, we consider as in [19] shortest-distance-based association strategy. Then, in each time slot $t \in \mathcal{T}$ the association variables $\alpha_{k,m}$ defined in Section III can be determined as

$$\alpha_{k,m} = \begin{cases} 1, & \text{if } k = \arg\min_k \|\mathbf{cod}_k^t - \mathbf{cod}_m\|^2 \\ 0, & \text{otherwise} \end{cases} . \quad (22)$$

Further divide the whole network area into a set of three dimensional rectangles. In each time slot, each UAV is allowed to either move to one of its adjacent rectangles or stay in the current. For each of the candidate rectangles, the UAV will first calculate the achievable capacity given the transmission power calculated in Sections IV-A and IV-B and the set of ground users it serves. Finally, as in [29], reinforcement learning with ϵ-greedy search is adopted to guide the exploitation and exploration during the UAV's flight control. The details of the learing algorithm are omitted due to space limitations.

D. Complexity Analysis

The most time-consuming operation in the above procedure is offline-dataset guided online power adaptation in Section IV-B. In Section IV-B1, we need to determine the network feature η^t given the UAV network's topology and the maximum tolerable SINR outage probability. Since the SINR outage probability is a monotonically increasing function of η^t, the value of η^t can be obtained efficiently based on bisection search. The dataset generation and regression in Section IV-B2 can be conducted offline, and in Section IV-B3 $\mathrm{Pr}_{\mathrm{Rx}}^{\max}$ can be determined online by solving a linear problem.

Regarding communication overhead, as illustrated in Fig. 1, in Section IV-A the AFC needs to collect one-time location and orientation information of the incumbent system and broadcast the collected information to the UAVs. If the incumbent system does not move frequently (which is usually the case, e.g., fixed point-to-point applications), the resulting communication overhead can be neglected. The AFC also needs to collect periodically the UAVs' locations and broadcast the updated power adaptation coefficient η^t to the UAVs. Since it is enough to represent these information in 16 bytes (three float numbers for location and one for the power adaptation coefficient, and each float number takes 4 bytes), the resulting broadcast overhead is low as well. Moreover, we will show later in Section V that the UAVs do not need to report their locations to the AFC in real-time, without obviously increasing the SINR outage probability of the incumbent system. This will further reduce the communication overhead.

V. Performance Evaluation

In this section we validate the effectiveness of the *SwarmShare* framework described in Sections III and IV. We consider a network area of $500 \times 500 \times 50$ m^3, with 50 ground users randomly located in the network and the number of UAVs varying from 3 to 24. The incumbent transmitter and receiver are deployed with coordinates of (200, 200, 10) and (250, 250, 10), respectively. The center frequency of the shared spectrum is set to 6 GHz with total bandwidth of 10 MHz. The maximum transmission power of the incumbent transmitter and the UAVs are set to 1 W and 0.25 W, respectively. For the bisectorized antenna model desribed in Section III, the maximum and minimum gains are set to 1 and 0.5, respectively. The power density of the AWGN is set to -174 dBm/Hz. The probability of LoS and NLoS links are set to 0.7 and 0.3, respectively. The threshold parameters $l_{\mathrm{euc}}^{\mathrm{th}}$ and $l_{\mathrm{hgh}}^{\mathrm{th}}$ in (15) are set to 70 m and 30 m, respectively. Next, before discussing the interference control results, we first determine the threshold angle for the directional antenna model described in Section III-B and validate the effectiveness of the data-driven calibration scheme proposed in Section IV-B.

Threshold Angle Measurement. We first determine the threshold angle for the directional antenna model described in Section III-B by conducting a set of experimental measurements. A snapshot of the testbed is shown in Fig. 2(a), where the transmitter is a USRP B210 software radio with omnidirectional antenna, the receiver is another USRP B210 with Tupavco TP542 antenna, and the baseband signal processing is conducted based on GNU Radio on a Dell Latitude 7400 laptop. Tupavco TP542 is a directional Wi-Fi antenna operating in frequency range up to 5.8 GHz (very close to the 6 GHz band) with antenna gain of 13 dBi. We measure the received power by varying the relative of the transmitter with respect to the boresight direction of the directional antenna (as illustrated in Fig. 2 (a)) and the transmission distance from 1 to 3 meters. Examples of the measurement results are given in Fig. 2(b) with transmission range of 1 m and relative angles varying from 0 to 120 degrees at step of 30 degrees. The mapping between the received power and relative angle is established based on logarithmic regression method [30]. Based on the regression results, we set 30 degree

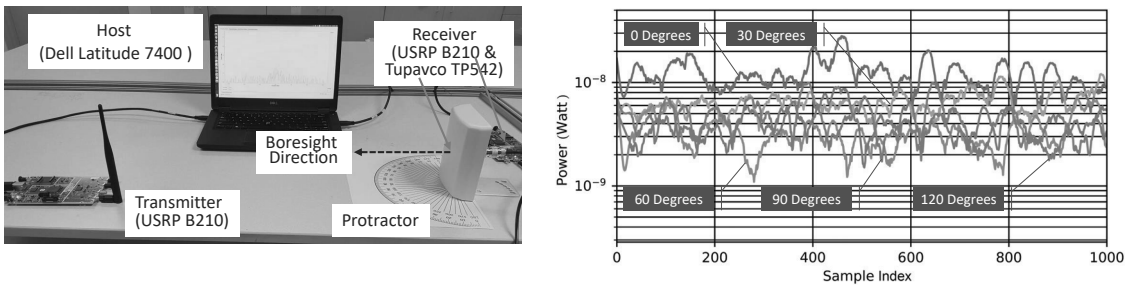

(a) (b)

Fig. 2: (a) Snapshot of the testbed setup for threshold angle measurement; (b) Examples of the measurement results.

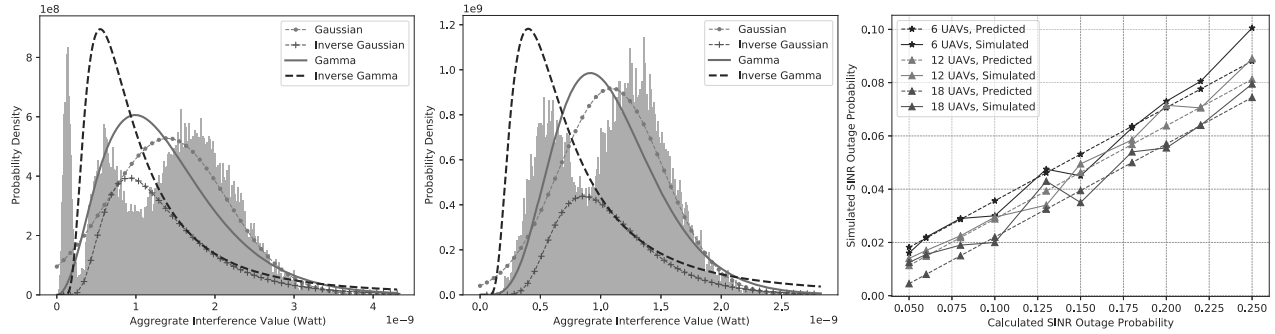

(a) (b) (c)

Fig. 3: Aggregate interference pdf with (a) 10 and (b) 20 UAVs; (c) Validation of data-driven predication of the SINR outage probability for the incumbent system.

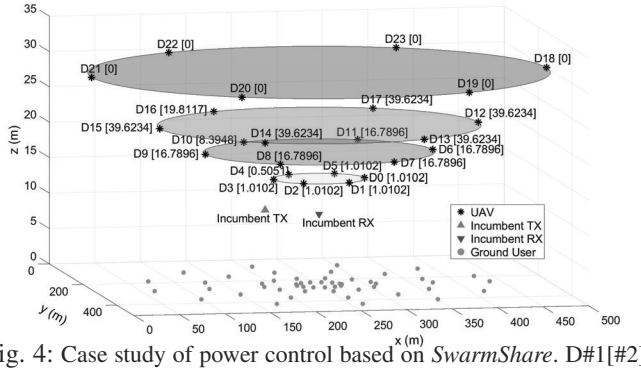

Fig. 4: Case study of power control based on *SwarmShare*. D#1[#2]: #1 is the UAV index, and #2 denotes the transmission power of the UAV in mW.

as the threshold angle for the bisectorized antenna model Section III-B, which corresponds to the 3 dB angle of the Tupavco TP542 antenna.

Data-driven Interference Prediction. Given the above obtained threshold angle, we further characterize the statistical behavior of the aggregate interference from the coexisting UAVs to the incumbent receiver. To this end, we conduct a set of simulations over UBSim, a newly developed Universal Broadband Simulator for integrated aerial-ground networking. Details of the simulator are omitted due to space limitations. The results are reported in Figs. 3(a) and (b) with 10 and 20 UAVs, respectively. We fit as in [31], [32] the collected interference values using four distributions, including Gaussian, Inverse Gaussian, Gamma and Inverse Gamma, and find that the power of the aggregate interference does not follow any of these distributions. This is actually our motivation to design *SwarmShare* based on a data-driven approach. Fig. 3(c) reports the results of the data-driven prediction of the SINR outage probability. We can find that the predicted SINR outage probability matches well the simulated.

Case Study. Figure 4 shows an example of the power control results based on *SwarmShare*. To visualize the effects of the power control principles described in Section IV-A, in this example all the 24 UAVs are deployed uniformlly along 4 circles with different altitudes and radiuses. From the figure it can be seen that lower transmission powers have been allocated to UAVs along the lower circles. Also, because of the shorter distances from the incumbent receiver, lower transmission power has been allocated to the UAVs of the first circle from the bottom, e.g., 1.0102 mW for UAV 1 (i.e., D1[1] in Fig. 4) against 16.7896 mW for UAV 7 and 39.6234 mW for UAV 13 along the second and third circles, respectively. Moreover, along the same circle UAVs more aligned with the incumbent receiver have been allocated lower transmission powers, e.g., 8.3948 mW for UAV 10 vs 39.6234 mW for UAV 9 along the second circle. Finally, we notice in this example that all the UAVs along the fourth (i.e., the highest) circle have been allocated zero transmission power because no users are associated with them based on the shortest-distance association strategy described in Section IV-C. This also conforms to the third power control principle, i.e., with the same distance and relative angle, higher altitudes result in lower transmission power because of higher probability of LoS transmissions. It is worth pointing out that the power allocation results are determined by jointly considering the three basic principles described in Section IV-A. In the following experiments, we will further evaluate the effectiveness of *SwarmShare* on the cross-system interference control.

In Figs. 5 and 6, we plot the instantaneous capacity achievable by the incumbent system and the UAV networks with different numbers of UAVs. In Fig. 5(a), we consider 6 hovering UAVs, and the maximum tolerable SINR outage probability is set to 0.05 for the incumbent system. The achievable capacity is plotted for 1000 time slots. Results indicate that the interference constraint of the incumbent system can be very well fulfilled, with SINR outage probability of 0.032. Similar results can be obtained with 12 and 18 hovering UAVs in Figs. 5(b) and (c), with the SINR outage probabilities of 0.029 and 0.021, respectively.

Figure 6 shows the corresponding results with moving UAVs. In this experiment, the network area is divided into a set of three-dimension rectangles each of $50 \times 50 \times 10$ m^3. The trajectory of the UAVs are controlled as described in Section IV-C, with exploitation probability of 0.98. The same as in Fig. 5, the incumbent system's interference constraints can be satisfied in all the tested cases, with SINR outage probability of 0.023, 0.019 and 0.018 for 6, 12 and 18 UAVs, respectively, all below the maximum tolerable outage probability 0.05. This verifies the effectiveness of *SwarmShare* in cross-system interference control.

Average Results. In Fig.7 we report the average capacity

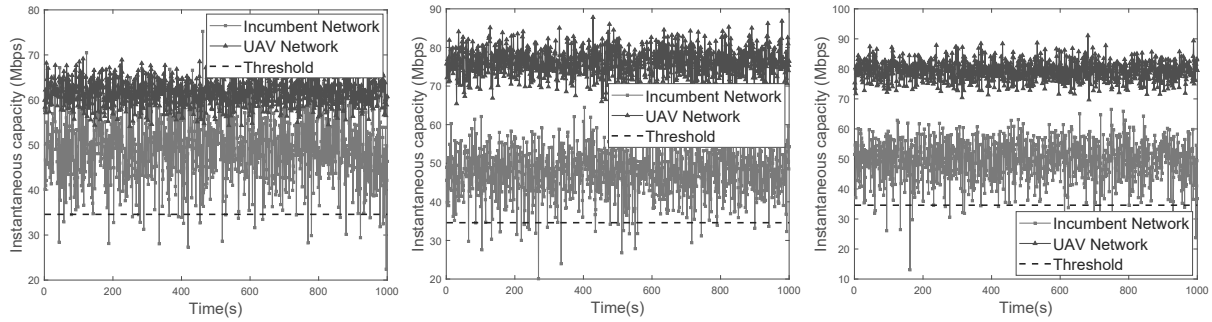

(a) 6 UAVs, Hovering (b) 12 UAVs, Hovering (c) 18 UAVs, Hovering

Fig. 5: Instantaneous capacity of the incumbent system and the UAV network with hovering UAVs. The violation probabilities are (a) 0.032, (b) 0.029 and (c) 0.021, respectively.

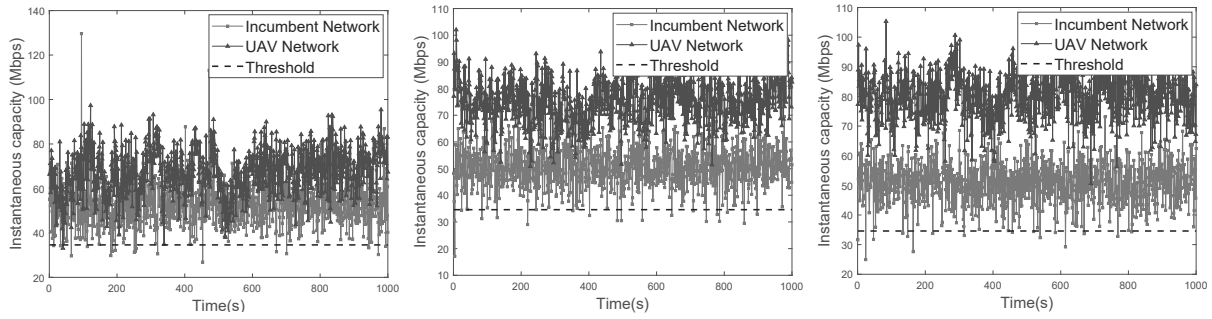

(a) 6 UAVs, Moving (b) 12 UAVs, Moving (c) 18 UAVs, Moving

Fig. 6: Instantaneous capacity of the incumbent system and the UAV network with moving UAVs. The violation probabilities are (a) 0.023, (b) 0.019 and (c) 0.018, respectively.

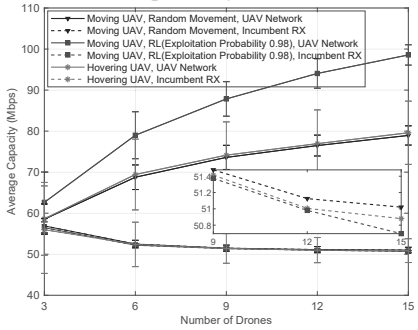

Fig. 7: Average capacity of the incumbent system and UAV networks with moving UAVs.

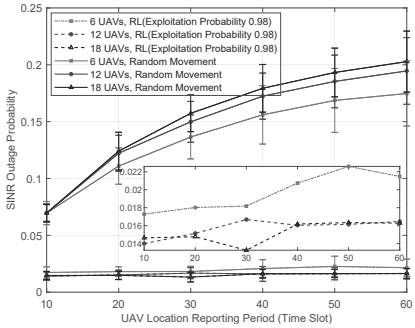

Fig. 8: SINR outage probability vs UAV location reporting period.

achievable by the incumbent system and the UAV network with the number of UAVs varying from 3 to 15 at step of 3. Three UAV motility patterns are considered: i) random movement; ii) reinforcement learning controlled movement with exploitation probability of 0.98; and iii) hovering UAVs. The resutls are obtained by averaging over 50000 time slots for each mobility pattern. It can be seen that, as expected, obvious capacity gain can be achieved by the UAV network with all the above three mobility patterns by deploying more UAVs. For example, for hovering UAVs, the average capacity increases from around 60 Mbps with 3 UAVs to 80 Mbps with 15 UAVs. The capacity is further increased to around 100 Mbps with RL-controlled UAV movement. Particularly, we find that there is no obvious degradation in the capacity of the incumbent system when there are 6 or more coexisting UAVs. The average capacity of the incumbent system can be further increased with less UAVs, e.g., 3, because of the reduced cross-system interference.

In previous experiments (i.e., Fig. 5) the UAVs report their locations to the AFC in every time slot. In this experiment, we investigate the mobility resilience of *SwarmShare* for spectrum sharing in the presence of inaccurate UAV locations. The SINR outage probability results are reported in Fig. 8, where two mobility patterns are considered for the UAVs, i.e., random movement and RL-guided movement, and the maximum tolerable SINR outage probability is set to 0.05 for the incumbent system. The location reporting period is varied from 10 time slots to 60. It can be seen that the SINR outage probability of the incumbent system increases monotonically with the location reporting period if the UAVs move in an uncontrolled manner, i.e., completely randomly. For example, the outage probability is around 0.07 when the reporting period is 10 time slots and can be up to 0.2 for 60 time slots. In the case of controlled UAV movement, the SINR outage

probability is barely affected by the location reporting period and always below the maximum tolerable. This is because the UAVs will stick with their current best locations at a high probability (0.98 in this experiment) while exploring new locations at a low probability (0.02). As a result, the topology of the UAV network and hence the statistical behavior of their aggregate interference to the incumbent system changes only slowly. Therefore, with controlled UAV movement, effective interference control can be achieved with *SwarmShare* in mobile scenarios even with inaccurate UAV locations, e.g., because of the temporary loss of the connections to the AFC.

VI. Conclusions

In this paper, we proposed a new framework called *SwarmShare* to enable spectrum sharing between the incumbent systems and the coexisting UAV networks in the 6 GHz band. We validated the effectiveness of the framework through an extensive simulation campaign. *SwarmShare* is shown to be mobility-resilient and hence is suitable for the operations of moving vehicles such as cars and UAVs on this newly opened spectrum band *without* requiring pre-defined exclusion zones. It is also found that the aggregate interference of the UAVs does not follow any existing distributions. In future work we will develop new theoretical models to characterize the aggregate interference of the UAVs and further validate the effectiveness of *SwarmShare* over the UAV testing facilities being developed in our lab.

References

[1] Z. Chu, W. Hao, P. Xiao, and J. Shi, "UAV Assisted Spectrum Sharing Ultra-Reliable and Low-Latency Communications," in *Proc. of IEEE GLOBECOM*, Waikoloa, USA, Dec. 2019.

[2] B. Shang, L. Liu, R. M. Rao, V. Marojevic, and J. H. Reed, "3D Spectrum Sharing for Hybrid D2D and UAV Networks," *IEEE Transactions on Communications*, vol. 68, no. 9, pp. 5375–5389, May 2020.

[3] "Unlicensed Use of 6 GHz Band," in *Notice of Proposed Rulemaking ET Docket No.18-295; GN Docket No. 17-183*, Oct. 2018.

[4] V. Sathya, M. I. Rochman, M. Ghosh, and S. Roy, "Standardization Advances for Cellular and Wi-Fi Coexistence in the Unlicensed 5 and 6 GHz Bands," *GetMobile*, vol. 24, no. 1, pp. 5–15, March 2020.

[5] B. Wang, Y. Sun, Z. Sun, L. D. Nguyen, and T. Q. Duong, "UAV-Assisted Emergency Communications in Social IoT: A Dynamic Hypergraph Coloring Approach," *IEEE Internet of Things Journal*, vol. 7, no. 8, pp. 7663–7677, April 2020.

[6] J. Lyu, Y. Zeng, and R. Zhang, "Spectrum Sharing and Cyclical Multiple Access in UAV-Aided Cellular Offloading," in *Proc. of IEEE GLOBECOM*, Singapore, January 2018.

[7] H. Wang, J. Wang, G. Ding, J. Chen, Y. Li, and Z. Han, "Spectrum Sharing Planning for Full-Duplex UAV Relaying Systems With Underlaid D2D Communications," *IEEE JSAC*, vol. 36, no. 9, pp. 1986–1999, August 2018.

[8] T. Q. Duong, L. D. Nguyen, H. D. Tuan, and L. Hanzo, "Learning-Aided Realtime Performance Optimisation of Cognitive UAV-Assisted Disaster Communication," in *Proc. of IEEE GLOBECOM*, Waikoloa, USA, February 2019.

[9] A. Fotouhi, H. Qiang, M. Ding, M. Hassan, L. G. Giordano, A. Garcia-Rodriguez, and J. Yuan, "Survey on UAV Cellular Communications: Practical Aspects, Standardization Advancements, Regulation, and Security Challenges," *IEEE Communications Surveys Tutorials*, vol. 21, no. 4, pp. 3417–3442, March 2019.

[10] M. Zareei, C. Vargas-Rosales, R. V. Hernndez, and E. Azpilicueta, "Efficient Transmission Power Control for Energy-harvesting Cognitive Radio Sensor Network," in *Proc. of IEEE International Symposium on PIMRC Workshops*, Istanbul, Turkey, Sept. 2019.

[11] Jie Xiang, Yan Zhang, and Tor Skeie, "Joint Admission and Power Control for Cognitive Radio Cellular Networks," in *Proc. of IEEE Singapore Int'l. Conference on Communication Systems*, Guangzhou, China, Jan. 2008.

[12] H. Guo, R. Long, and Y. Liang, "Cognitive Backscatter Network: A Spectrum Sharing Paradigm for Passive IoT," *IEEE Wireless Communications Letters*, vol. 8, no. 5, pp. 1423–1426, Oct. 2019.

[13] M. Labib, A. F. Martone, V. Marojevic, J. H. Reed, and A. I. Zaghloul, "A Stochastic Optimization Approach for Spectrum Sharing of Radar and LTE Systems," *IEEE Access*, vol. 7, pp. 60 814–60 826, April 2019.

[14] C. Aydogdu *et al.*, "RadChat: Spectrum Sharing for Automotive Radar Interference Mitigation," *IEEE Transactions on Intelligent Transportation Systems*, vol. 22, no. 1, pp. 416–429, December 2021.

[15] A. F. Martone, K. A. Gallagher, and K. D. Sherbondy, "Joint Radar and Communication System Optimization for Spectrum Sharing," in *Proc. of IEEE Radar Conference (RadarConf)*, Boston, USA, April 2019.

[16] M. L. Attiah, A. A. M. Isa, Z. Zakaria, M. Abdulhameed, M. K. Mohsen, and I. Ali, "A Survey of mmWave User Association Mechanisms and Spectrum Sharing Approaches: An Overview, Open Issues and Challenges, Future Research Trends," *Wireless Networks*, vol. 26, no. 4, pp. 2487–2514, 2020.

[17] J. Ren, Y. He, G. Huang, G. Yu, Y. Cai, and Z. Zhang, "An Edge-Computing Based Architecture for Mobile Augmented Reality," *IEEE Network*, vol. 33, no. 4, pp. 162–169, January 2019.

[18] J. Cui, Y. Liu, and A. Nallanathan, "Multi-Agent Reinforcement Learning-Based Resource Allocation for UAV Networks," *IEEE Trans. on Wireless Communications*, vol. 19, no. 2, pp. 729–743, August 2020.

[19] S. K. Moorthy and Z. Guan, "FlyTera: Echo State Learning for Joint Access and Flight Control in THz-enabled Drone Networks," in *Proc. of IEEE SECON*, Como, Italy, June 2020.

[20] L. Bertizzolo, E. Demirors, Z. Guan, and T. Melodia, "CoBeam: Beamforming-based Spectrum Sharing with Zero Cross-Technology Signaling for 5G Wireless Networks," in *Proc. of IEEE INFOCOM*, Toronto, Canada, July 2020.

[21] Y. Li, H. Zhang, K. Long, S. Choi, and A. Nallanathan, "Resource Allocation for Optimizing Energy Efficiency in NOMA-based Fog UAV Wireless Networks," *IEEE Network*, vol. 34, no. 2, pp. 158–163, September 2020.

[22] N. Vervliet, O. Debals, L. Sorber, and L. De Lathauwer, "Breaking the Curse of Dimensionality Using Decompositions of Incomplete Tensors: Tensor-based Scientific Computing in Big Data Analysis," *IEEE Signal Processing Magazine*, vol. 31, no. 5, pp. 71–79, August 2014.

[23] K. T. Hemachandra and N. C. Beaulieu, "Novel Representations for the Equicorrelated Multivariate Non-Central Chi-Square Distribution and Applications to MIMO Systems in Correlated Rician Fading," *IEEE Trans. on Commun.*, vol. 59, no. 9, pp. 2349–2354, March 2011.

[24] S. Kusaladharma and C. Tellambura, "Aggregate Interference Analysis for Underlay Cognitive Radio Networks," *IEEE Wireless Communications Letters*, vol. 1, no. 6, pp. 641–644, December 2012.

[25] A. A. Khuwaja, Y. Chen, and G. Zheng, "Effect of User Mobility and Channel Fading on the Outage Performance of UAV Communications," *IEEE Wireless Commun. Letters*, vol. 9, no. 3, pp. 367–370, March 2020.

[26] A. F. Schmidt and C. Finan, "Linear Regression and the Normality Assumption," *Journal of clinical epidemiology*, vol. 98, pp. 146–151, June 2018.

[27] S. K. Moorthy and Z. Guan, "Beam Learning in MmWave/THz-band Drone Networks Under In-Flight Mobility Uncertainties," *IEEE Transactions on Mobile Computing*, accepted for publication, Oct. 2020.

[28] H. Zhang, N. Yang, W. Huangfu, K. Long, and V. C. M. Leung, "Power Control Based on Deep Reinforcement Learning for Spectrum Sharing," *IEEE Transactions on Wireless Communications*, vol. 19, no. 6, pp. 4209–4219, June 2020.

[29] S. A. Al-Ahmed, M. Z. Shakir, and S. A. R. Zaidi, "Optimal 3D UAV Base Station Placement by Considering Autonomous Coverage Hole Detection, Wireless Backhaul and User Demand," *Journal of Commun. and Networks*, vol. 22, no. 6, pp. 467–475, December 2020.

[30] D. W. Hosmer Jr, S. Lemeshow, and R. X. Sturdivant, *Applied Logistic Regression*. USA: John Wiley & Sons, 2013.

[31] Z. Guan, T. Melodia, and G. Scutari, "To Transmit or Not to Transmit? Distributed Queueing Games for Infrastructureless Wireless Networks," *IEEE/ACM Trans. on Netw.*, vol. 24, no. 2, pp. 1153–1166, April 2016.

[32] R. K. Ganti and M. Haenggi, "Interference in Ad Hoc Networks with General Motion-Invariant Node Distributions," in *Proc. of IEEE Int'l. Symposium on Information Theory*, Toronto, Canada, July 2008.